

# A Diffusion Filter for Discontinuous Surface Measured by High Definition Metrology

Meng Wang<sup>1,#</sup>, Yi-Ping Shao<sup>1</sup>, Shi-Chang Du<sup>1,2</sup>, and Li-feng Xi<sup>1,2</sup>

<sup>1</sup> School of Mechanical Engineering, Shanghai Jiao Tong University, Shanghai, 200240, China

<sup>2</sup> State Key Laboratory of Mechanical System and Vibration, Shanghai, 200240, China

# Corresponding Author / E-mail: mwang@sjtu.edu.cn, TEL: +86-021-34206783

KEYWORDS: Surface quality, Areal surface texture, Discontinuous surface, Diffusion filter, High definition metrology

*High definition metrology can measure three-dimensional surface topography of discontinuous surfaces that have holes and grooves with large field of field and high lateral resolution. However, when separating discontinuous surfaces in to various scale-limited surface such as form, waviness and roughness, filtering techniques such as Gaussian filters cause "boundary distortion problems. This is because the discontinuous surfaces do not have large enough continuous evaluation area for Gaussian filtering. Therefore, this research proposes a modified anisotropic diffusion filter, which is formulated in terms of heat diffusion, to separate discontinuous surfaces into various scale-limited surfaces. An edge detector is proposed to ensure that the diffusion process only takes place inside the surface but not blur the surface boundaries. In addition, the diffusion time is specified considering the linkage with the cutoff wavelength of Gaussian filters. The performance of the proposed filter is validated by simulated and practical discontinuous surfaces. Moreover, the three dimensional areal surface texture features specified in ISO 25178 can be evaluated from the filtered scale-limited surfaces. Results have demonstrated that the proposed approach is an effective tool for separating and evaluating areal surface texture for discontinuous surfaces regardless of the continuity of the evaluation surface.*

Manuscript received: January 30, 2015 / Accepted: June 16, 2015

## 1. Introduction

Discontinuous surfaces are machined engineering surfaces with holes and grooves, such as the engine block faces, the engine desk faces, automatic transmission valve joint surfaces, and torque converter housing surfaces (as shown in Fig 1(a)-1(d)). As surface quality is directly related to mechanical properties and functional attributes,<sup>1</sup> the evaluation of three-dimensional surface texture (or areal surface texture in other words) for discontinuous surfaces has gained increasing significance in manufacturing.

Measuring the three-dimensional surface topography of discontinuous surfaces needs large field of view and high lateral resolution. A novel non-contact metrology called high definition metrology (HDM) meets such requirements. HDM can measure the three-dimensional surface topography of engineering surface with 0.15 mm lateral resolution in lateral direction and 1  $\mu$ m accuracy in depth direction, and can generate millions of data points.<sup>2</sup> Unlike the areal surface texture measuring techniques such as those areal-topography techniques and areal-integrating techniques mentioned in ISO 25178-6,<sup>3</sup> HDM can measure entire surface instead of a local area. Therefore, HDM provides new

possibilities for 3D surface texture evaluation of the discontinuous surfaces. However, in spite of the development of measurement metrology, there is limited research that addresses the evaluation of discontinuous surfaces.

Filtering techniques are well established to separate the measured surface into various scale-limited surfaces for further analysis. Then, surface features including form, waviness and roughness can be calculated from the large, medium, and small scale surface. Nevertheless, traditional filters such as Gaussian filters are only appropriate for continuous surfaces that do not have nonempty data within the evaluation area. As for discontinuous surfaces, Gaussian filters cause "boundary distortion or end effects problems due to surface discontinuity caused by empty data at the hole areas. Although adding extra data points such as zero padding or extrapolation is a possible way for signal processing, it may be inaccurate for surface texture evaluation.

Specifically, take for example the filtering of HDM measured automobile engine block face (Fig. 2). With the roughness and waviness specifications  $Rz=12.5$ ,  $R_{max}=15$ , and  $Wt=10$ , the cutoff wavelengths of roughness are 0.008 mm and 2.5 mm, and the cutoff wavelengths of

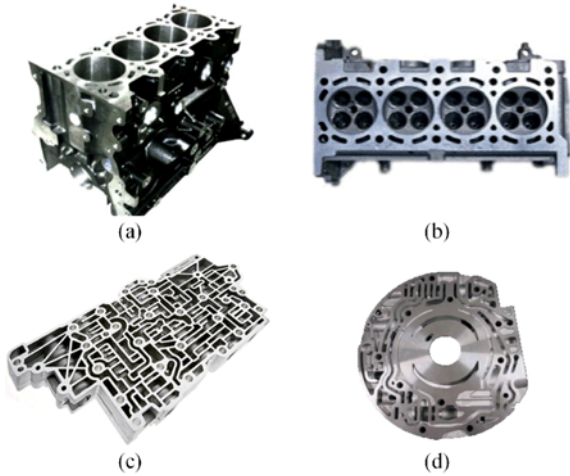


Fig. 1 Examples of discontinuous engineering surfaces

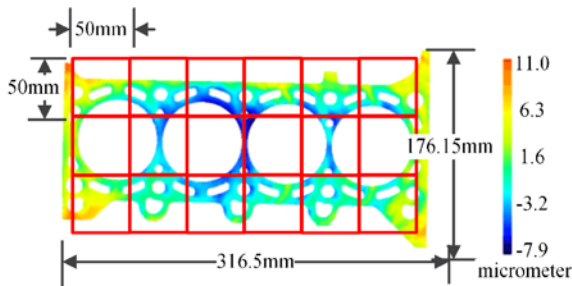


Fig. 2 Engine block face measured by HDM

waviness are 2.5 mm and 25 mm, respectively.<sup>4</sup> Therefore, the HDM data contains the 3D surface form and 3D surface waviness information (HDM cannot measure roughness due to the lateral resolution). To separate waviness from surface form using Gaussian filtering, the minimum traversing length should include half a waviness cutoff on each end of the evaluation length according to ASME B46.1<sup>5</sup> to reduce the end effects, which means the traverse should be at least twice the long-cutoff wavelength of waviness, i.e. 50 mm. However, for engine block faces with cylinder holes, bolt holes and cooling holes, there is no 50 mm × 50 mm continuous evaluation area (as shown in red boxes of Fig. 2). Therefore, the surface texture at the boundaries of the holes will be distorted. Consequently, it is difficult to evaluate 3D surface texture of discontinuous surfaces.

To overcome the problem of edge distortions, as well as outlier-induced distortions, new filters such as robust Gaussian filters,<sup>6</sup> robust spline filters,<sup>7</sup> wavelet filters,<sup>8</sup> and shearlet filters<sup>9</sup> have been proposed. The progress on filtration in surface metrology is illustrated in a thorough review by Jiang, X. J. and Whitehouse, D. J..<sup>10</sup> Among these new filters, the anisotropic diffusion filter is worth exploring due to its edge preserving abilities. Anisotropic diffusion filters, which are formulated in terms of heat diffusion process, have been successfully developed for image edge detection in which the image intensity can only diffuse inside of the objects but not across the boundaries. Therefore, the image objects are smoothed without blurring their boundaries.

Recently, anisotropic diffusion filters have been adopted for the filtering of structured engineering surfaces that have deterministic structure with high aspect ratio geometric features. Zeng et al. employed the diffusion filter for MEMS surfaces.<sup>11</sup> Jiang et al. adopted the diffusion filter for freeform engineering surfaces.<sup>12</sup> The features of MEMS surface and freeform surfaces are well preserved with high accuracy. However, for discontinuous surfaces, the boundaries of the objects are known in advance. Therefore, we propose a modified anisotropic diffusion filter by adding edge detectors to stop any diffusion across the boundaries. Section 2 introduces the details of the modified anisotropic diffusion filter and the parameters setting criteria for practical use. Section 3 demonstrates the effectiveness of the modified anisotropic diffusion filter on a simulated discontinuous surface. In Section 4, an experiment on engine block faces is conducted and the areal surface texture is calculated. Finally, Section 5 draws the conclusions.

## 2. Diffusion Filtering

In this section, a modified anisotropic diffusion filter with edge detectors is presented for the filtering of discontinuous engineering surfaces.

### 2.1 Anisotropic diffusion filtering

The anisotropic diffusion filter comes from the heat diffusion equation which describes the changes of heat within a specified region with respect to time and space. The general model of the diffusion equation is:

$$\frac{\partial u}{\partial t} = \text{div}(c\nabla u) \quad (1)$$

where  $u$  is the quantity of interest,  $\text{div}$  is the divergence operator,  $\nabla$  is the gradient operator, and  $c$  stands for the conduction function, which is a measurement of the diffusion speed. If  $c$  is constant, the diffusion process is isotropic.

Perona, P. and Malik, J. first applied anisotropic diffusion process to digital image by introducing an adaptive conduction function  $c = g(|\nabla u_t|^2)$ , where  $u_t$  represents the image intensity at time  $t$  and  $g$  is a function of the Euclidean magnitude of the gradient of  $u_t$ .<sup>13</sup> It represents that the diffusion speed is adaptive according to the gradient. Specifically, the diffusion speed is quick within the interior region where the gradient is small and slow at the boundaries where the gradient is large. Therefore, the function  $g$  should be a nonnegative monotonically decreasing function of the gradient. Two typical formulations for conduction function  $g$  are:

$$g_1 = \exp(-|\nabla u_t|^2 / K^2) \quad (2)$$

$$g_2 = 1 / (1 + |\nabla u_t|^2 / K^2) \quad (3)$$

where parameter  $K$  controls the direction of the diffusion process. The regions with gradient smaller than  $K$  are smoothed; the regions with gradient larger than  $K$  are enhanced.  $K$  can either be a value depending on the gradient or set by hand. Weickert J. proposed a different conduction function in which the diffusion speed is much more rapid

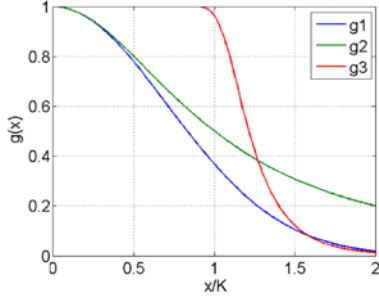


Fig. 3 Three conduction functions

in the interior region.<sup>14</sup>

$$g_3 = \begin{cases} 1 - \exp(-3.315/(\nabla u/K)^8) & , |\nabla u| \neq 0 \\ 1 & , |\nabla u| = 0 \end{cases} \quad (4)$$

Fig. 3 illustrates the three conduction functions. It can be seen that  $g_3$  is much larger than  $g_1$  and  $g_2$  for  $|\nabla u|/K < 1$ . As the it is calculated at each iteration, the conduction coefficient depends on both space variables and time variable.

The diffusion filter needs to be discretized for practical use. Let  $I(i, j)$  be the surface height at location  $(i, j)$  at time zero,  $I_{i,j}^{t+1}$  be the diffused surface height at location  $(i, j)$  and time  $t$ . The discrete scheme of the anisotropic diffusion filter is as follows:<sup>13</sup>

$$I_{i,j}^{t+1} = I_{i,j}^t + \lambda [c_N \nabla_N I + c_S \nabla_S I + c_E \nabla_E I + c_W \nabla_W I]_{i,j}^t \quad (5)$$

$$I_{i,j}^0 = I(i, j)$$

where  $0 \leq \lambda \leq 1/4$  for the scheme to be stable, the subscripts  $N, S, E, W$  are the abbreviation of North, South, East, and West. The symbol  $\nabla$  here indicates the difference between each pixel and its nearest neighbors in four directions:

$$\begin{aligned} \nabla_N I_{i,j}^t &= I_{i-1,j}^t - I_{i,j}^t & \nabla_S I_{i,j}^t &= I_{i+1,j}^t - I_{i,j}^t \\ \nabla_E I_{i,j}^t &= I_{i,j+1}^t - I_{i,j}^t & \nabla_W I_{i,j}^t &= I_{i,j-1}^t - I_{i,j}^t \end{aligned} \quad (6)$$

The conduction coefficients are updated at each iteration:

$$\begin{aligned} c_{N,i,j}^t &= g(|\nabla_N I_{i,j}^t|) & c_{S,i,j}^t &= g(|\nabla_S I_{i,j}^t|) \\ c_{E,i,j}^t &= g(|\nabla_E I_{i,j}^t|) & c_{W,i,j}^t &= g(|\nabla_W I_{i,j}^t|) \end{aligned} \quad (7)$$

## 2.2 Anisotropic diffusion filter with edge detectors

One major difference between the filtering of discontinuous surfaces and structured engineering surfaces is that the surface boundary of the former is already known in advance. Therefore, we can completely prevent the diffusion across the boundaries by setting the conduction coefficient equal to zero at the boundary. Specifically, if two adjacent points both belong to the surface, diffusion can take place between them. Otherwise, diffusion between two empty points or between one empty point and one boundary point is prohibited. This is achieved by edge detectors  $W_N, W_S, W_E, W_W$ . First, let  $w_{i,j}$  be the window function of the discontinuous surface.  $w_{i,j}=1$  if  $I_{i,j}$  belong to the surface, otherwise  $w_{i,j}=0$ . Therefore, the edge detectors are defined as follows:

$$\begin{aligned} W_{N,i,j} &= w_{i-1,j} \cdot w_{i,j} & W_{S,i,j} &= w_{i+1,j} \cdot w_{i,j} \\ W_{E,i,j} &= w_{i,j+1} \cdot w_{i,j} & W_{W,i,j} &= w_{i,j-1} \cdot w_{i,j} \end{aligned} \quad (8)$$

Hence, the anisotropic diffusion filter with edge detectors is

$$I_{i,j}^{t+1} = I_{i,j}^t + \lambda [W_N c_N \nabla_N I + W_S c_S \nabla_S I + W_E c_E \nabla_E I + W_W c_W \nabla_W I]_{i,j}^t \quad (9)$$

The diffused surface is deemed as the areal form, and difference between the original surface and diffused surface is the areal surface texture.

## 2.3 Parameters setting

When calculating the conduction function  $g$ , smoothing the gradient with a kernel can eliminate noise.<sup>15</sup> However, to avoid any possible edge distortion, the original gradient is used without smoothing.

The coefficient  $K$  in the condition function can be chosen as the mean absolute value of the gradient for MEMs surfaces<sup>11</sup> or 70% percentile of the gradient histogram for image segmentation.<sup>16</sup> However, to allow smoothing within the interior surface,  $K$  is chosen as the maximum gradient within the surface:

$$K = \max(|W_N \nabla_N I|, |W_S \nabla_S I|, |W_E \nabla_E I|, |W_W \nabla_W I|) \quad (10)$$

To be consistent with Gaussian filters, the time  $t$  should be assigned carefully. The two-dimensional areal Gaussian filter is:

$$S(x, y) = \frac{1}{\alpha^2 \lambda^2} \exp\left[-\frac{\pi(x^2 + y^2)}{\alpha^2 \lambda^2}\right] \quad (11)$$

where  $\alpha = \sqrt{\ln 2 / \pi}$ , and  $\lambda$  is the cutoff wavelength in  $x$  and  $y$  directions. The relation between the standard error of the Gaussian filter  $\sigma$  and cutoff wavelength  $\lambda$  is:

$$\sigma = \frac{\alpha}{\sqrt{2\pi}} \lambda = \sqrt{\frac{\ln 2}{2}} \frac{\lambda}{\pi} \quad (12)$$

Let  $\sigma_1$  denote the standard deviation in pixels, and  $l$  denote the sampling distance between two adjacent pixels. Therefore,  $\sigma_1$  is given by:

$$\sigma_1 = \frac{\sigma}{l} \quad (13)$$

A linkage exists between Gaussian filter and diffusion filter. In the case of the Gaussian scale space, the convolution of an image with a Gaussian kernel of standard deviation  $\sigma_1$  is equivalent to diffuse the image for some time  $t$  with the following correspondence:<sup>16</sup>

$$t = \sigma_1^2 / 2 \quad (14)$$

Note that Eq. (13) does not indicate a theoretical relation between the Gaussian filter of standard deviation  $\sigma_1$  and the diffusion filter of time  $t$ . Nevertheless, it provides a sound basis for practical use. Combining the Eqs. (12) to (14) gives the relation between diffusion time  $t$  and Gaussian cutoff wavelength  $\lambda$ :

$$t = \frac{\ln 2}{4\pi^2} \left(\frac{\lambda}{l}\right)^2 = 0.0176 \left(\frac{\lambda}{l}\right)^2 \quad (15)$$

## 3. Simulation

A discontinuous areal surface is simulated to evaluate the performance of the proposed filter:

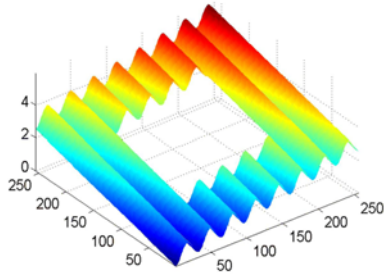


Fig. 4 Simulated discontinuous surface

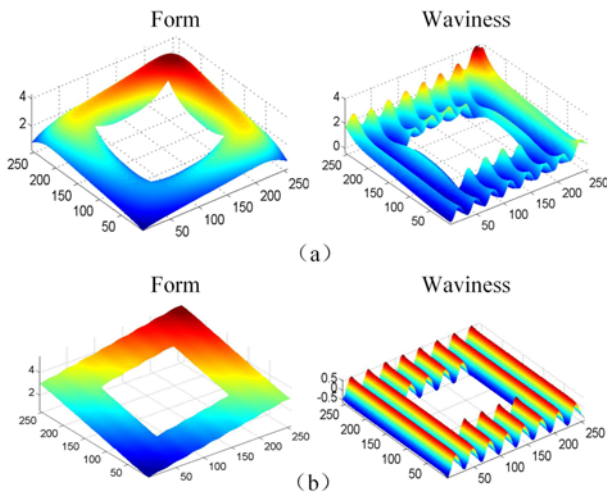


Fig. 5 Filtered surface form and waviness: (a) Gaussian filter, (b) diffusion filter

$$z(x,y) = -0.5\cos(2\pi x/6.4) + 0.05x + 0.05y \quad (16)$$

The cosine term is regarded as surface waviness and last two terms are regarded as the surface form. The wavelength of surface waviness is 6.4 mm. The area of the simulated surface is 51.2 mm × 51.2 mm. The sampling spacing is  $l = 0.2$  mm in  $x$  and  $y$  directions. The simulated surface has 256×256 data points. To simulate the discontinuous surface, a square area in the center is removed (as shown in Fig. 4).

Gaussian filter and the proposed anisotropic diffusion filter are applied to the simulated surface, respectively. The cutoff wavelength for Gaussian filter is 25 mm. For the diffusion filter, conduction function  $g_3$  is used and the corresponding diffusion time is  $t = 0.0176(25/0.2) = 275$ . The filtered results are displayed in Fig. 5.

The Gaussian filtered surface form and waviness show serious end effects near the inner and outer boundaries. In practice use, half of the cutoff wavelength is discarded at the boundaries. However, the simulated discontinuous surface can not afford the boundary removal due to the small evaluation area. On the other hand, the areal surface form and waviness are separated satisfactorily with no boundary distortion by diffusion filtering.

The root mean square error of the difference between the diffusion filtered waviness and nominal cosine surface is calculated. Fig. 6 shows the plot of root mean square error versus diffusion time  $t$ . It can be seen

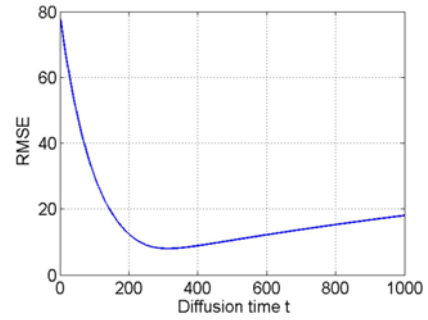


Fig. 6 Plot of the root mean square error versus diffusion time

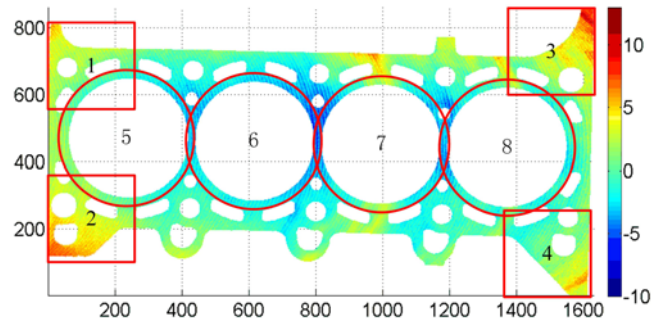


Fig. 7 Eight regions for areal surface texture evaluation

that the root mean square error reaches its minimum around the time 275, which implies that the setting of diffusion time is reasonable.

#### 4. Experiment

An experiment on the face milling process of engine blocks was conducted to demonstrate the ability of the proposed filter for practical surfaces. The depth of cut was 0.5 mm, the cutting speed was 1300 rpm, and feed rate was 3360 mm/min. The face-milling cutter had a diameter of 200 mm with 15 cutting inserts intercalated by three wiper inserts. The finished engine block faces were measured by HDM. Raw HDM data was converted into grid image with resampling interval  $l = 0.2$  mm using the HDM data preprocessing method proposed by Wang et al.<sup>17</sup>

Fig. 7 displays the HDM converted image of the engine block face. Eight regions are selected to evaluate the areal surface texture. From Fig. 7 we can see that the four corner areas of the engine block face have large surface variation, so square regions with an area of 50 mm × 50 mm at the four corners are selected as region 1 to region 4. Moreover, the surface texture around the cylinder bore has vital influence on the sealing performance, so region 5 to region 8 are circular regions around the cylinder bore with a radius of 80 mm.

ISO 25178 is the latest geometrical product specification standard on areal surface texture. In ISO 25178, F-filter is used to remove surface form from the primary surface. As HDM data contains surface form information and surface the waviness, the diffusion filtering is applied only once as the F-filter to separate surface waviness and surface form. As the waviness cutoff is 25 mm, the diffusion time is  $t = 275$ .

Table 1 Calculated areal surface textures

	$S_q$	$S_{sk}$	$S_{ku}$	$S_p$	$S_v$	$S_z$	$S_a$
Region 1	0.74	-0.01	3.04	3.26	4.29	7.55	0.59
Region 2	0.63	-0.10	3.22	2.69	3.88	6.57	0.50
Region 3	0.82	-0.01	3.22	3.27	4.02	7.29	0.65
Region 4	0.74	-0.01	3.04	3.26	4.29	7.55	0.59
Region 5	0.78	0.05	2.92	3.19	3.40	6.59	0.63
Region 6	0.77	0.03	2.98	2.93	3.29	6.22	0.62
Region 7	0.81	0.07	2.97	4.14	4.24	8.38	0.65
Region 8	0.90	0.09	3.03	3.79	3.82	7.61	0.72

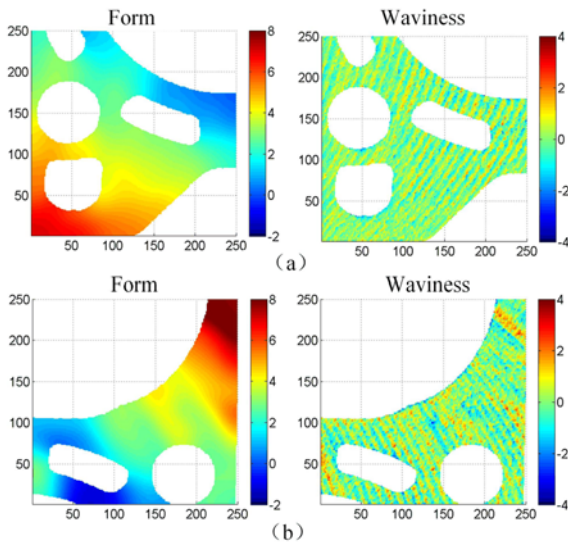


Fig. 8 Filtered square regions: (a) region two, (b) region three

Conduction function  $g_3$  is used and  $K$  is set as the maximum gradient within each region. To begin with, the proposed diffusion filter is performed on the eight regions to acquire the surface form. Then the filtered surfaces are subtracted from the raw surface to generate areal surface waviness. Finally, based on the filtered primary surface, we calculate the height parameters in ISO 25178-2<sup>18</sup> including root mean square height  $S_q$ , skewness  $S_{sk}$ , kurtosis  $S_{ku}$ , maximum peak height  $S_p$ , maximum pit height  $S_v$ , maximum height  $S_z$ , and arithmetical mean height  $S_a$ .

Table 1 shows the calculated height parameters of the areal waviness of the eight regions. The dimension is micrometer.

As can be observed from Table 1, region 2 and region 3 have the minimum and maximum  $S_q$  and  $S_a$  among the four square regions. The diffusion filtered surface form and waviness of region 2 and region 3 are illustrated in Fig. 8. Similarly, the diffusion filtered surface form and waviness of region 6 and region 8 are presented in Fig. 9. It can be seen that the areal waviness are separated accurately from the surface form at these regions.

Region 8 has the largest  $S_q$  and  $S_a$  value of the four circular regions, which may imply the sealing performance of the cylinder bore at this region could be worse than the other three. In light of this, evaluation of local areal surface texture at critical areas and global areal texture over the entire surface are both suggested to access the susceptibility to leakage of combustion gases, coolant or lubricant.

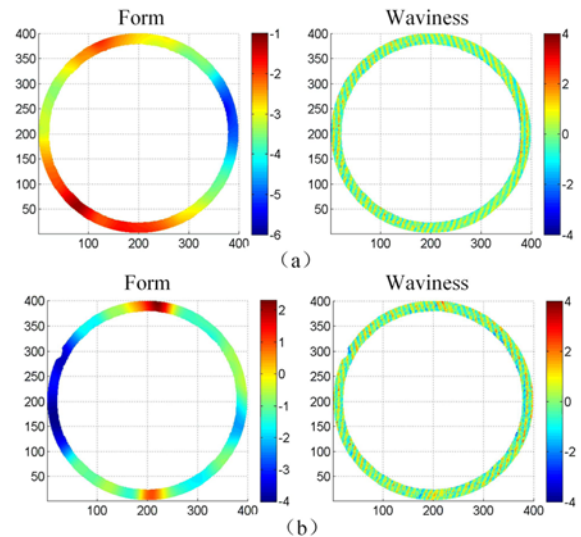


Fig. 9 Filtered circular regions: (a) region six, (b) region eight

## 5. Conclusions

In this study, a modified anisotropic diffusion filter is introduced to filter discontinuous engineering surfaces into various scale-limited surfaces. The edge detector is adopted to ensure that the diffusion process will only take place inside the surface but not across the boundaries. The diffusion time is specified considering its relation with the cutoff wavelength of Gaussian filters. Simulated and experimental discontinuous surfaces demonstrate that the proposed anisotropic diffusion filter can separate areal surface waviness from areal surface form accurately. Thus, three dimensional surface texture parameters instead of the two dimensional surface texture can be calculated based on the filtered surface, which helps fully evaluate the surface quality and functional performance.

In future work, we plan to focus on the consistency between diffusion filter and Gaussian filters for different simulated and practical discontinuous surfaces.

## ACKNOWLEDGEMENT

This work is supported by the National Science & Technology Pillar Program of China (2012BAF06B03), the National Natural Science Foundation of China (51275558), the Programme of Introducing Talents of Discipline to Universities (B06012), the Fund for Innovative Research Groups of the National Natural Science Foundation of China (51121063), and Shanghai Rising-Star Program (Grant No. 13QA1402100). We are grateful to engineers in SAIC GM Wuling Automobile for their support on experiments.

## REFERENCES

1. Kamguem, R., Tahan, S. A., and Songmene, V., "Evaluation of Machined Part Surface Roughness using Image Texture Gradient Factor," Int. J. Precis. Eng. Manuf., Vol. 14, No. 2, pp. 183-190,



- 2013.
2. Huang, Z., Shih, A.J., and Ni, J., "Laser Interferometry Hologram Registration for Three-Dimensional Precision Measurements," *Journal of Manufacturing Science and Engineering*, Vol. 128, No. 4, pp. 1006-1013, 2006.
  3. ISO 25178-6, "Geometrical Product Specifications (GPS) - Surface Texture: Areal - Part 6: Classification of Methods for Measuring Surface Texture," 2010.
  4. ISO 4288, "Geometrical Product Specifications (GPS) - Surface Texture: Profile Method - Rules and Procedures for the Assessment of Surface Texture," 1996.
  5. AME B46.1, "Surface Texture (Surface Roughness, Waviness, and Lay)," 2009.
  6. Seewig, J., "Linear and Robust Gaussian Regression Filters," *Journal of Physics: Conference Series*, Vol. 13, pp. 254-257, 2005..
  7. Goto, T., Miyakura, J., Umeda, K., Kadowaki, S., and Yanagi, K., "A Robust Spline Filter on the Basis of  $l_2$ -Norm," *Precision Engineering*, Vol. 29, No. 2, pp. 157-161, 2005.
  8. Zeng, W., Jiang, X., and Scott, P., "Metrological Characteristics of Dual-Tree Complex Wavelet Transform for Surface Analysis," *Measurement Science and Technology*, Vol. 16, No. 7, pp. 1410-1417, 2005.
  9. Du, S., Liu, C., and Huang, D., "A Shearlet-based Separation Method of 3D Engineering Surface using High Definition Metrology," *Precision Engineering*, Vol. 40, pp. 55-73, 2015.
  10. Jiang, X. J. and Whitehouse, D. J., "Technological Shifts in Surface Metrology," *CIRP Annals-Manufacturing Technology*, Vol. 61, No. 2, pp. 815-836, 2012.
  11. Zeng, W., Jiang, X., Scott, P. J., and Blunt, L., "Diffusion Filtration for the Evaluation of Mems Surface," *Proc. of the 10th International Symposium of Measurement Technology and Intelligent Instruments*, 2011.
  12. Jiang, X., Cooper, P., and Scott, P. J., "Freeform Surface Filtering using the Diffusion Equation," *Proceedings of the Royal Society of London A: Mathematical, Physical and Engineering Sciences*, pp. 841-859, 2011.
  13. Perona, P. and Malik, J., "Scale-Space and Edge Detection using Anisotropic Diffusion," *IEEE Transactions on Pattern Analysis and Machine Intelligence*, Vol. 12, No. 7, pp. 629-639, 1990.
  14. Weickert, J., "Efficient Image Segmentation using Partial Differential Equations and Morphology," *Pattern Recognition*, Vol. 34, No. 9, pp. 1813-1824, 2001.
  15. Alvarez, L., Lions, P.-L., and Morel, J.-M., "Image Selective Smoothing and Edge Detection by Nonlinear Diffusion. II," *SIAM Journal on Numerical Analysis*, Vol. 29, No. 3, pp. 845-866, 1992.
  16. Alcantarilla, P. F., Bartoli, A., and Davison, A. J., "Kaze Features," *Computer Vision-ECCV 2012*, pp. 214-227, 2012.
  17. Wang, M., Xi, L., and Du, S., "3d Surface Form Error Evaluation using High Definition Metrology," *Precision Engineering*, Vol. 38, No. 1, pp. 230-236, 2014.
  18. ISO 25178-2, "Geometrical Product Specifications (GPS) - Surface Texture: Areal - Part 2: Terms," *Definitions and Surface Texture Parameters Surface Texture*, 2012.